*Progress In Electromagnetics Research C, Vol. 51, 35–43, 2014*

# A Novel Single Feed Omnidirectional Circularly Polarized Antenna with Wide AR Bandwidth

**Long Yang*, Neng-Wu Liu, Zhi-Ya Zhang, Guang Fu, Qiong-Qiong Liu, and Shao-Li Zuo**

**Abstract**—A novel omnidirectional circularly polarized (CP) antenna with single feed is proposed for 2.4 GHz WLAN applications. Based on the zeroth-order resonance (ZOR) mode of epsilon negative (ENG) transmission line (TL), the antenna excites uniform vertically polarized $E$-field just as the monopole does. A modified Alford loop with electromagnetic coupling fed by L-shaped strip consists of four curved branches, which is placed on the top of the antenna and generates an equivalent horizontally polarized magnetic dipole mode. Once the two orthogonally polarized components are equal in amplitude but different in phase by 90°, omnidirectional CP wave can be obtained. The measured results show that the impedance bandwidth ($S_{11} < -10$ dB) is 6% (2.38–2.53 GHz), and the 3-dB axial ratio bandwidth in the azimuth plane is very wide which achieves 54% (1.60–2.80 GHz). Additionally, the 3-dB axial ratio beamwidth is over 50° for radiation pattern in elevation plane. Moreover, the antenna achieves excellent omnidirectional right-hand CP performance with a variation of 0.5 dB in the azimuth plane and an average gain over 1.5 dB across the operating band, which are well applied to the wireless system.

## 1. INTRODUCTION

In recent years, omnidirectional CP antennas have attracted more and more attention due to their advantages and wide use in different applications. For omnidirectional CP antennas, when transmitting and receiving signals, it is relatively insensitive to their respective orientations, and they can contemporaneously suppress the effect of multi-path reflections of waves caused by the nearby objects [1]. Thus, the omnidirectional CP antennas are very useful for various wireless systems such as global positioning system, radio frequency identification, and wireless local area network [2–4]. To meet the rapidly increased requirements for wireless systems, many omnidirectional CP antennas have been proposed by using helical antenna [5], spiral patch-slot antenna [6] and bended monopoles [7, 8]. An easy and common way to design an omnidirectional CP antenna is to achieve two fields orthogonal both in space and time from an electric dipole and a magnetic dipole just by a single feeding line. A uniform vertically polarized component against ground plane can be generated by top-loaded cylindrical monopole [9] or a metamaterial antenna which is called zeroth-order resonance antenna [10–12]. They always have mushroom patch and can achieve omnidirectional performance. A horizontally polarized component can be obtained by omnidirectional magnetic dipole which can be realized by the arc-shaped dipoles or by an Alford loop antenna and its variants [13–15]. In [9], the proposed antenna consists of a top-loaded cylindrical monopole and four printed arc-shaped dipoles to obtain CP wave, and the 90° phase difference can be achieved by adjusting the diameter of the ground. The impedance and AR bandwidth are narrow which can just cover the WLAN band. In [16], the CP antenna uses an arc-shaped mushroom structure with curved branches to radiate CP wave, but its impedance and AR bandwidth are less than 5%. In [17], the Alford loop of the proposed design is excited through the coupling

*Received 14 April 2014, Accepted 28 May 2014, Scheduled 15 June 2014*

* Corresponding author: Long Yang (wuyanqianzi@163.com).

The authors are with the Science and Technology on Antenna and Microwave Laboratory, Xidian University, Xi'an 710071, People's Republic of China.

between the patch and dielectric resonator. This feature improves the AR bandwidth to 8%. Another omnidirectional CP dielectric resonator antenna with parasitic strips provides a wide AR bandwidth of more than 20% [18].

In this paper, we present a novel compact omnidirectional CP antenna with wide axial ratio bandwidth and high RHCP gain. The antenna consists of four curved branches which are electromagnetic coupling fed by L-shaped strips, four shorting pins and a rectangular patch fed by the coaxial pin in the middle. The curved branches constitute the modified Alford loop, which generate horizontally polarized component. Meanwhile, the vertically polarized component can be generated by ZOR mode of the antenna. The 90° phase difference between the two polarizations is naturally provided by the antenna. Finally, the antenna achieves a measured impedance bandwidth for $S_{11} < -10$ dB of 6% (2.38–2.53 GHz) and 3-dB axial ratio bandwidth of 54% (1.60–2.80 GHz) in the azimuth plane. The proposed antenna has a compact size with a dimension of $0.4\lambda \times 0.4\lambda \times 0.08\lambda$. Furthermore, the antenna achieves a high RHCP gain. The designed antenna has been fabricated, and the experimental results are discussed.

## 2. ANTENNA DESIGN AND DISCUSSION

Figure 1 shows the configuration of the proposed antenna. As shown in Figure 1(a), it mainly consists of four curved branches with shorting pins, a rectangular patch with four L-shaped strips and a ground plane. The ground and upper patch are printed on the bottom and top substrates, respectively, and both of the substrates have a relative permittivity of 2.65 and thickness of 1 mm. Utilizing the epsilon negative (ENG) transmission line (TL), the antenna generates ZOR mode to achieve vertically polarized component. The modified Alford loop which produces horizontally polarized component consists of four curved branches fed by L-shaped strips with electromagnetic coupling method. What is worth mentioning is that the electromagnetic coupled feeding significantly enhances the 3-dB AR bandwidth which achieves about 80% (1.5–3.5 GHz). The 90° phase difference between the vertical and horizontal polarizations is intrinsically provided by the zeroth-order resonator. Additionally, the coaxial feed is placed at the center of the rectangular patch, as shown in Figure 1(b). Therefore, the antenna has an omnidirectional CP radiation pattern in the azimuth plane, because each curved branch distributed centrosymmetrically has the same field distribution. The final optimal antenna parameters are shown in Table 1.

To confirm the principle of the omnidirectional CP antenna, the electric field and current distribution are simulated using HFSS 14. According to the simulated results, both the vertically and horizontally polarized $E$-fields can be generated, shown in Figure 2. As shown in Figure 2, the

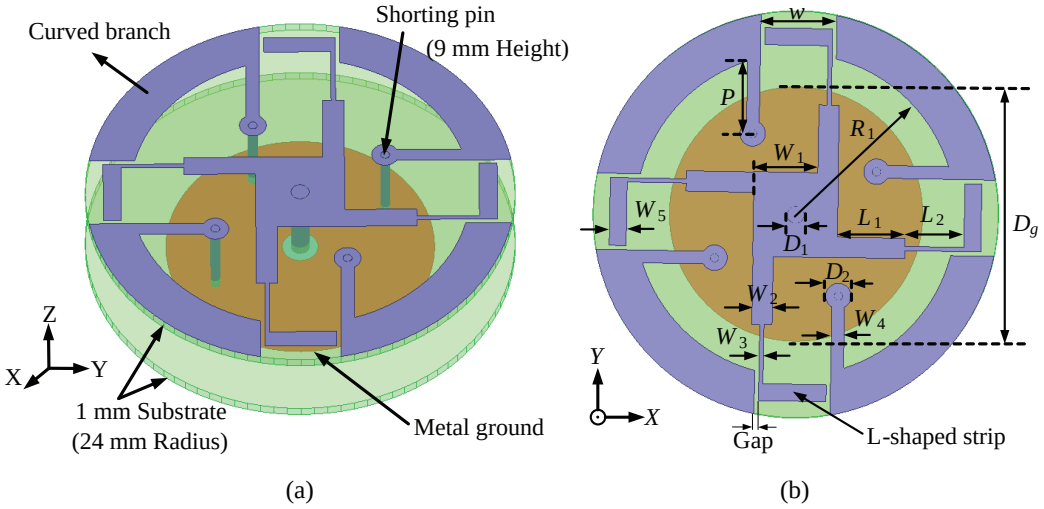


**Figure 1.** Geometry of the proposed design. (a) 3-D view. (b) Top view.

electric field (on the left) and surface surface current (on the right) distribution of the CP antenna are plotted in a period of time ($T$). Here, we divide $T$ into four moments, $t = 0$, $t = T/4$, $t = T/2$, and $t = 3T/4$. For Figures 2(a) and (b) ($t = 0$), the horizontally polarized component generated by flowing current ($J_\Phi$) on the curved branches is much greater than the vertically polarized component, thus, it mainly radiates horizontally polarized wave at this time. At $t = T/4$, the current on the curved branches can be neglected when compared with the vertically polarized component ($E_\theta$), thus, the vertical polarized $E$-field domains at this moment. Actually, the $E$-fields at $t = 0$ and $t = T/4$ are dominated by the magnetic-monopole mode of the modified Alford loop and the electric-monopole mode of the ZOR antenna, respectively. It can be seen that the two $E$-fields are orthogonal both in space and time. Similarly, when it comes to $t = T/2$ and $t = 3T/4$, the antenna mainly radiates reversely polarized wave with respect to the horizontally polarized wave in Figure 2(b) and vertically polarized wave in Figure 2(c), respectively. Therefore, the resonator of ENG TL inherently provides a 90° phase difference between two orthogonal components for the reason that it behaves as a capacitor and keeps a charged and discharged state periodically. Note that the vertically polarized $E$-field ($E_\theta$) always delays 90 degrees in phase compared with the horizontally polarized component generated by the flowing current ($J_\Phi$) on the curved branches in a period of time $T$, resulting in a right-hand CP characteristic of the antenna. Conversely, if the direction of arrangement of four curved branches is in the clockwise direction, the left-hand CP characteristic will be obtained. Additionally, when the antenna parts which affect the horizontally and vertically polarized waves are adjusted well to guarantee the equal magnitude, a good circular polarization performance can be obtained.

Theoretically, wavelength for the resonant frequency at 2.45 GHz is calculated by the expression:

$$L = \frac{c}{4f\sqrt{\dfrac{\varepsilon_r + 1}{2}}}$$

According to this expression, $L$ is 22 mm. The shorting pins and curved branches are the dominative resonant parts when the antenna works at 2.45 GHz, which means that the resonant wavelength is the total length of the two parts which is about 24 mm, and it has been marked in Figure 2(b) by A → B → C → D. Thus, the simulated resonant wavelength agrees well with the theoretical one for the frequency at 2.45 GHz.

It is observed that the electromagnetic coupling feed has significant effects on the VSWR and AR bandwidth enhancement. To investigate the influence of the related geometrical dimensions on the proposed antenna performance, analysis on the key parameters of the curved branches is discussed. Figures 3 and 4 show the simulated VSWR and axial ratio bandwidth responses of the curved branches with different lengths ($W$) and gaps (Gap) between the branches and the inverted L-shaped strips when other parameters are fixed to the values listed in Table 1.

Figure 3 shows the simulated VSWR and AR ($\theta = 90°$, $\Phi = 0°$) as functions of frequency for different lengths of curved branch which is described by the parameter $W = 6$, 7.5, 9, 10 mm. The greater value $W$ represents, the shorter length the branch has. It can be noted from Figure 3(a) that the resonant frequency shifts to the lower frequency as $W$ decreases. The reason lies in the basic principle of LC resonance: the longer length of the branch is, the greater capacitance the antenna achieves, thus the resonant frequency decreases. Figure 3(b) shows the effect of the branch length on the AR. It can be seen that this parameter mainly affects the AR in the lower band. With increasing $W$, the AR in the lower band can be improved, thus, a wider AR bandwidth can be obtained. However, the AR in the middle band is extremely deteriorated when $W$ continues to increase. So, an optimum value of $w$ is chosen as 7.5 mm at the working frequency of 2.442 GHz.

**Table 1.** Dimensions of the proposed antenna.

| Parameters | $W$ | $W_1$ | $W_2$ | $W_3$ | $W_4$ | $P$ | $D_g$ |
|---|---|---|---|---|---|---|---|
| Values/mm | 7.5 | 7.6 | 2.4 | 0.5 | 1.5 | 8 | 30 |
| Parameters | $W_5$ | $L_1$ | $L_2$ | $R_1$ | $D_1$ | $D_2$ | Gap |
| Values/mm | 2 | 8 | 7 | 19 | 2 | 3 | 0.5 |

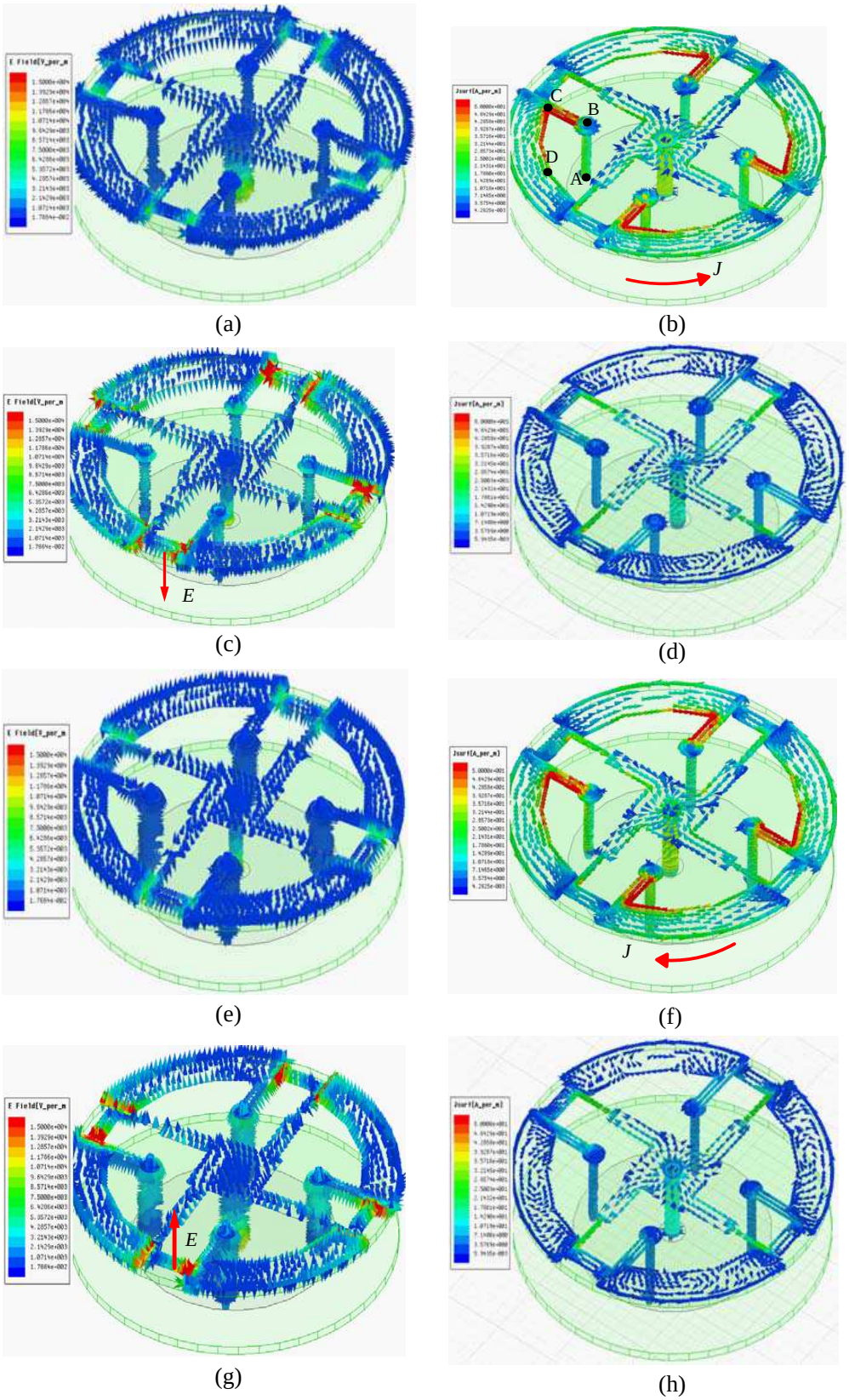


(a) (b) (c) (d) (e) (f) (g) (h)

**Figure 2.** (a), (c), (e), (g) Electric field and (b), (d), (f), (h) surface current distribution of the proposed antenna. (a), (b) $t = 0$, (c), (d) $t = T/4$, (e), (f) $t = T/2$, (g), (h) $t = 3T/4$.

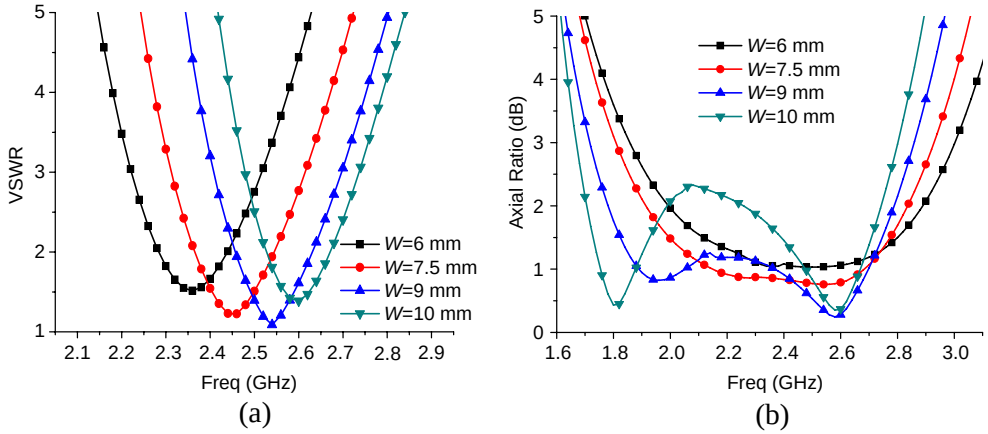


**Figure 3.** Effect of different curved branch lengths on (a) VSWR, (b) AR ($\theta = 90°$, $\Phi = 0°$).

Next, the effect of the gap between the curved branch and the L-shaped feeding strip on the antenna performance for Gap = 0.2, 0.5, and 0.8 mm is investigated, as shown in Figure 4. The AR bandwidth decreases when the gap becomes narrower. It can be noted that this parameter mainly affects the AR of the upper band, while the AR ($\theta = 90°$, $\Phi = 0°$) in the lower band changes slightly. This can be expected that the gap significantly affects the energy coupling between the branch and the L-shaped feeding strip, hence affecting the amplitude of the horizontally polarized $E$-field which is generated by the modified Alford-loop current in the upper band. With regard to VSWR, the resonant frequency slightly shifts to lower frequency as Gap decreases, because of a greater capacitor obtained.

Another important effect on the antenna performance is also studied and given by the position of the shorting pins. With reference to Figure 5, the resonant frequency shifts towards the lower frequency with a longer distance between the curved branches and the shorting pins, since a longer resonant length is obtained when $P$ increases. It is observed that this parameter affects the AR ($\theta = 90°$, $\Phi = 0°$) significantly. When $P$ increases, a wider AR bandwidth can be achieved. However, there is a trend that the AR in the middle band will dramatically increase when $P$ decreases continuously. The optimum value of $P$ is 8 mm. Therefore, apart from the Alford-loop parameters, the position of shorting pins can be used to optimize the impedance and AR bandwidths. The result shows that the AR can be optimized first, and then the matching can be achieved by simply varying the parameters of the curved branches and the position of the shorting pins without affecting the optimized AR.

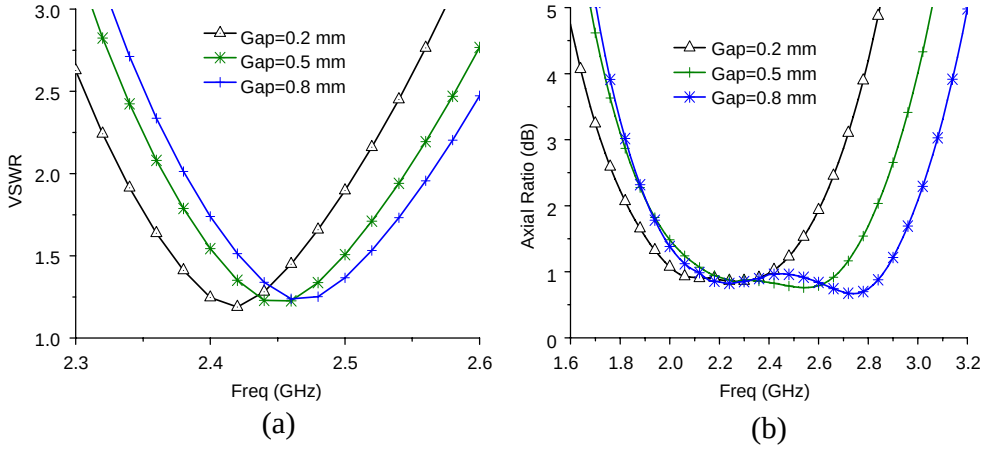


**Figure 4.** Figure 4. Effect of different gaps between the curved branch and the L-shaped strip on (a) VSWR, (b) AR ($\theta = 90°$, $\Phi = 0°$).

## 3. EXPERIMENTAL RESULTS

A prototype of the proposed antenna was fabricated according to the design parameters in Table 1. The measurements were carried out using Agilent E8363B network analyzer and an anechoic chamber. A bazooka balun which is used in the measurement to suppress the current through the outside conductor

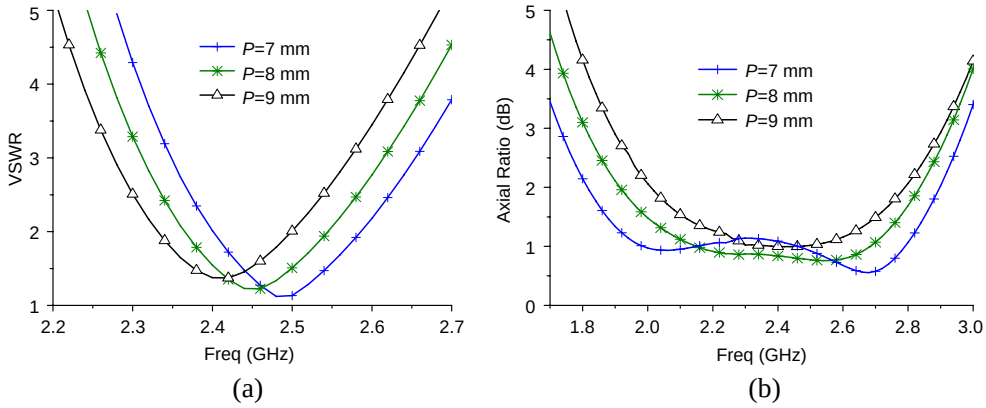


**Figure 5.** Effect of different position of the shorting pins on (a) VSWR, (b) AR ($\theta = 90°$, $\Phi$=0°).

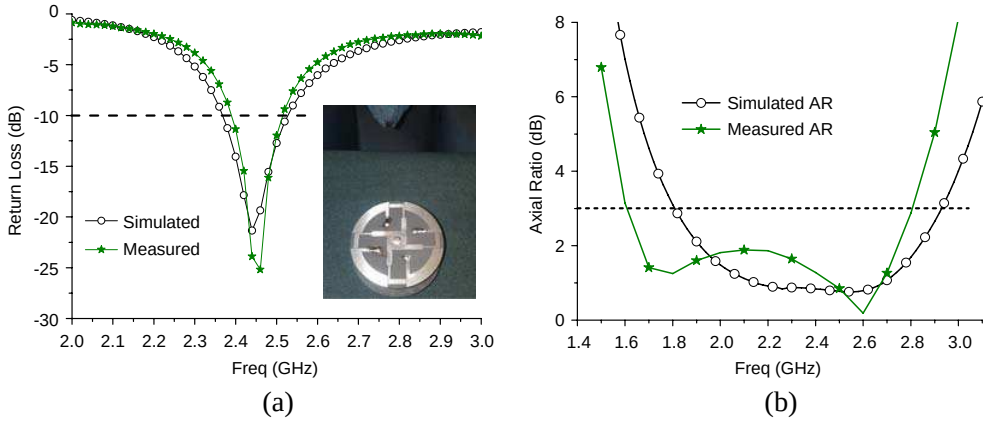


**Figure 6.** Measured and simulated RL and AR. (a) RL, (b) AR ($\theta = 90°$, $\Phi = 0°$).

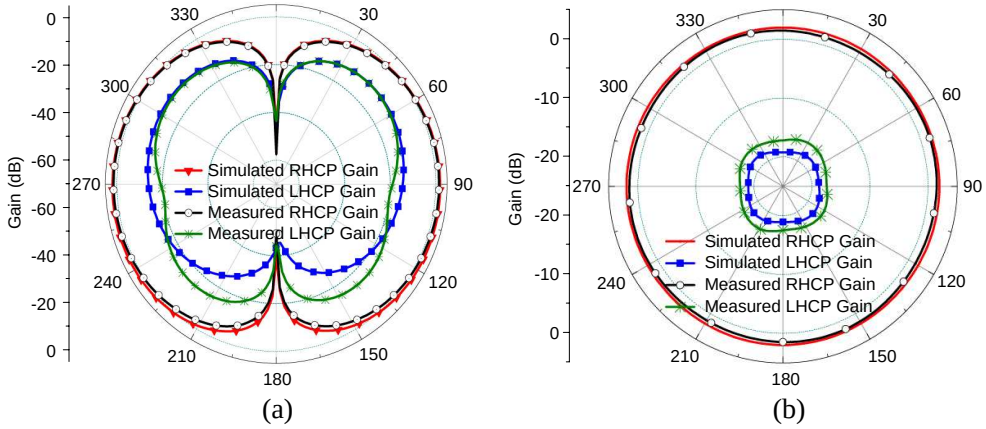


**Figure 7.** Simulated and measured patterns of the proposed antenna at 2.442 GHz. (a) Elevation ($x$-$z$) plane. (b) Azimuth ($x$-$y$) plane.

of coaxial cable is placed between the feeding port of the antenna and the connecting coaxial cable. Figure 6 presents the simulated and measured return loss and AR against the frequency for the proposed antenna. The measured impedance bandwidth which is about 6% (2.38–2.53 GHz) for $S_{11} < -10$ dB is slightly narrower than simulated one. But it can clearly cover the required bandwidth of the WLAN band (2.4–2.484 GHz). The AR was measured and simulated in the $+x$ direction ($\theta = 90°$, $\Phi = 0°$). As can be observed from Figure 6(b), the simulated and measured 3-dB AR bandwidths are 49% (1.80–2.95 GHz) and 54% (1.60–2.80 GHz), respectively. The measured result shows that the AR bandwidth is much wider than the impedance bandwidth, and the proposed CP antenna has excellent CP performance in the WLAN band.

Figure 7 shows the simulated and measured far field radiation patterns at 2.442 GHz, and both the azimuth and elevation planes of the patterns look quite monopole-like, and the difference is that the proposed antenna radiates circularly polarized wave when compared with the classical monopole. The simulated and measured RHCP gains are 1.95 dB and 1.52 dB, respectively. The discrepancy between the simulated and measured results is due to the fabrication error. Additionally, the difference between the RHCP and LHCP gains is larger than 15 dB. These results prove that the designed antenna radiates great RHCP wave. Radiation patterns at other frequencies are also explored, and they are very stable across the WLAN band.

Figure 8 shows the simulated and measured axial ratios of the antenna at 2.442 GHz at elevation ($X$-$Z$) and azimuth ($X$-$Y$) planes, respectively. In Figure 8(a), the measured 3 dB AR beamwidth at elevation plane is about 50° (70°–120°) which is narrower than simulated (70°–130°) as shown in the blue color. It can be explored from Figure 8(b) that the simulated and measured axial ratios at

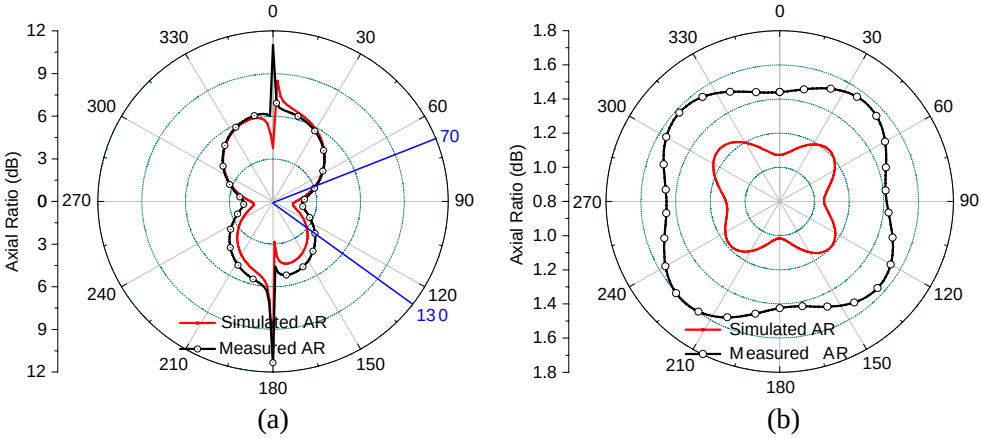


**Figure 8.** Simulated and measured axial ratio of the antenna at 2.442 GHz. (a) Elevation ($x$-$z$) plane. (b) Azimuth ($x$-$y$) plane.

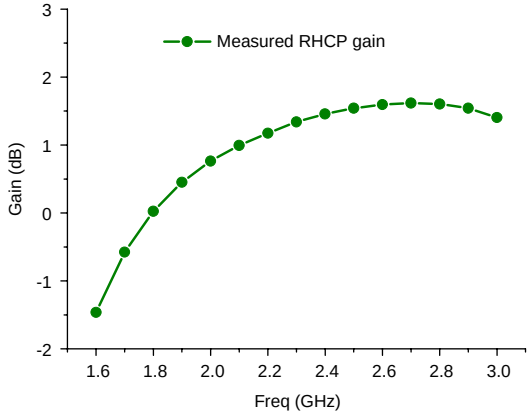


**Figure 9.** Measured RHCP gain in the $+x$ direction ($\theta = 90°$, $\Phi = 0°$) versus frequency.

2.442 GHz are 1.1 dB (the ripples are less than 0.2 dB) and 15 dB (the ripples are less than 0.2 dB), respectively. These results show that the proposed antenna exhibits an acceptable omnidirectional circularly polarized performance in the elevation plane. Figure 9 shows the measured antenna gain in the $+x$ direction ($\theta = 90°$, $\Phi = 0°$) versus frequency. With reference to the figure, the measured average RHCP gain is around 1.5 dB across the WLAN band. It is seen that the antenna in the operating band exhibits small (lower than 1.5 dB) and symmetric axial ratios (the ripples are less than 0.2 dB), which shows excellent omnidirectional CP property in the azimuth plane.

## 4. CONCLUSION

A novel omnidirectional CP antenna based on the modified Alford loop structure and epsilon negative transmission line is presented in the paper. By employing curved branches in the radiating patch edges, CP property and omnidirectional radiation performance are achieved. Measured results show that the AR bandwidth is 54% (1.60–2.80 GHz) with the help of electromagnetic coupling feed. Moreover, the measured RHCP gain is above 1.5 dB. Furthermore, the beamwidth of RHCP is about 50° (70°–120°) in the elevation plane, and the impedance bandwidth is about 6% (2.38–2.53 GHz) for $S_{11} < -10$ dB. Thus the antenna can cover the required bandwidth of the WLAN band. All of them illustrate that the novel antenna is valuable in wireless communication for its low profile simple structure.

## ACKNOWLEDGMENT

The authors would like to thank Professor Guang Fu for valuable suggestions. This work was supported by the Fundamental Research Funds for the Central Universities (Nos. K5051302033 and K5051307009).

## REFERENCES

1. Qian, Z. H., "Analysis of circularly polarized dielectric resonator antenna excited by a spiral slot," *Progress In Electromagnetics Research*, Vol. 47, 111–121, 2004.
2. Mak, K. M. and K. M. Luk, "A circularly polarized antenna with wide axial ratio beamwidth," *IEEE Trans. Antennas Propag.*, Vol. 57, No. 10, 3309–3312, Oct. 2009.
3. Yang, S. S., K.-F. Lee, A. A. Kishk, and K.-M. Luk, "Design and study of wideband single feed circularly polarized microstrip antennas," *Progress In Electromagnetics Research*, Vol. 80, 45–61, 2008.
4. Heidari, A. A., M. Heyrani, and M. Nakhkash, "A dual-band circularly polarized stub loaded microstrip patch antenna for GPS applications," *Progress In Electromagnetics Research*, Vol. 92, 195–208, 2009.
5. Wheeler, H. A., "A helical antenna for circular polarization," *Proc. IRE*, Vol. 35, No. 12, 1484–1488, Dec. 1947.
6. Cao, W. Q., A. J. Liu, B. N. Zhang, T. B. Yu, and Z. P. Qian, "Dual-band spiral patch-slot antenna with omnidirectional CP and unidirectional CP properties," *IEEE Trans. Antennas Propag.*, Vol. 61, No. 4, 2286–2289, Apr. 2013.
7. Kawakami, H. and R. Wakabayashi, "Research on circularly polarized conical beam antennas," *IEEE Trans. Antennas Propag.*, Vol. 39, No. 3, 27–39, Jun. 1997.
8. Yu, Y. F., S. L. He, and Z. X. Shen, "Electrically small omnidirectional antenna of circular polarization," *2012 IEEE Antennas and Propagation Society International Symposium (APSURSI)*, 1–2, 2012.
9. Hsiao, F. R. and K. L. Wong, "Low-profile omnidirectional circularly polarized antenna for WLAN access point," *Microw. Opt. Technol. Lett.*, Vol. 46, No. 3, 227–231, 2005.
10. Lee, J. G. and J. H. Lee, "Zeroth order resonance loop antenna," *IEEE Trans. Antennas Propag.*, Vol. 55, No. 3, 994–997, 2007.
11. Park, J. H., Y. H. Ryu, and J. H. Lee, "Epsilon negative zeroth order resonator antenna," *IEEE Trans. Antennas Propag.*, Vol. 55, No. 12, 3710–3712, 2007.

12. Yoo, S. and S. Kahng, "CRLH ZOR antenna of a circular microstrip patch capacitively coupled to a circular shorted ring," *Progress In Electromagnetics Research C*, Vol. 25, 15–26, 2012.
13. Wei, K. P., Z. J. Zhang, Z. H. Feng, and M. F. Iskander, "A MNG-TL loop antenna array with horizontally polarized omnidirectional patterns," *IEEE Trans. Antennas Propag.*, Vol. 60, No. 6, 2702–2710, Jun. 2012.
14. Alford, A. and A. G. Kandoian, "Ultra-high frequency loop antenna," *Electrical Engineering*, Vol. 59, No. 12, 843–848, 1940.
15. Lin, C. C., L. C. Kuo, and H. R. Chuang, "A horizontally polarized omnidirectional printed antenna for WLAN applications," *IEEE Trans. Antennas Propag.*, Vol. 54, No. 11, 3551–3556, Nov. 2006.
16. Park, B.-C. and J.-H. Lee, "Omnidirectional circularly polarized antenna utilizing zeroth-order resonance of epsilon negative transmission line," *IEEE Trans. Antennas Propag.*, Vol. 59, No. 7, 2717–2721, Jul. 2011.
17. Li, W. W. and K. W. Leung, "Omnidirectional circularly polarized dielectric resonator antenna with top-loaded Alford loop for pattern diversity design," *IEEE Trans. Antennas Propag.*, Vol. 61, No. 8, 4246–4256, Aug. 2013.
18. Pan, Y. M. and K. W. Leung, "Wideband omnidirectional circularly polarized dielectric resonator antenna with parasitic strips," *IEEE Trans. Antennas Propag.*, Vol. 60, No. 6, 2992–2997, Jun. 2012.